Atmos. Chem. Phys., 18, 1863–1877, 2018
https://doi.org/10.5194/acp-18-1863-2018
© Author(s) 2018. This work is distributed under
the Creative Commons Attribution 3.0 License.

Atmospheric Chemistry and Physics
Open Access

The effects of El Niño–Southern Oscillation on the winter haze pollution of China

Shuyun Zhao[2,3], **Hua Zhang**[1,2,3], **and Bing Xie**[2,3]

[1]Department of Atmospheric Science, School of Environmental Studies, China University of Geosciences, Wuhan, China
[2]Collaborative Innovation Center on Forecast and Evaluation of Meteorological Disasters, Nanjing University of Information Science and Technology, Nanjing, China
[3]Laboratory for Climate Studies, National Climate Center, China Meteorological Administration, Beijing, China

Correspondence: Hua Zhang (huazhang@cma.cn)

Received: 31 May 2017 – Discussion started: 22 June 2017
Revised: 7 December 2017 – Accepted: 11 December 2017 – Published: 8 February 2018

Abstract. It has been reported in previous studies that El Niño–Southern Oscillation (ENSO) influenced not only the summer monsoon, but also the winter monsoon over East Asia. This contains some clues that ENSO may affect the winter haze pollution of China, which has become a serious problem in recent decades, through influencing the winter climate of East Asia. In this work, we explored the effects of ENSO on the winter (from December to February) haze pollution of China statistically and numerically. Statistical results revealed that the haze days of southern China tended to be fewer (more) than normal in El Niño (La Niña) winter, whereas the relationships between the winter haze days of northern and eastern China and ENSO were not significant. Results from numerical simulations also showed that ENSO influenced the winter atmospheric anthropogenic aerosol content over southern China more obviously than it did over northern and eastern China. Under the emission level of aerosols for the year 2010, winter atmospheric anthropogenic aerosol content over southern China was generally greater (less) than normal in El Niño (La Niña) winter. This was because the transport of aerosols from South and Southeast Asia to southern China was enhanced (weakened), which masked the better (worse) scavenging conditions for aerosols in El Niño (La Niña) winter. The frequency distribution of the simulated daily surface concentrations of aerosols over southern China indicated that the region tended to have fewer clean and moderate (heavy) haze days, but more heavy (moderate) haze days in El Niño (La Niña) winter.

1 Introduction

Haze pollution, especially in winter, has become a very serious problem for China in recent decades (Ding and Liu, 2014; Tao et al., 2016). For example, in January 2013, most parts of central and eastern China experienced extremely heavy and persistent haze pollution (Tao et al., 2014; Mu and Zhang, 2014; Zhang et al., 2014b; Wang et al., 2014a, b; Zou et al., 2017). In the last decade, haze pollution in winter has received wide concern from the scientific community, the government of China, and the public.

Haze pollution is a phenomenon mainly caused by human-emitted pollutants under stagnant meteorological conditions. The increase in anthropogenic emissions of aerosols and their precursors in recent decades has been the main reason for the worsening air quality in China (Cao et al., 2007; Zhang et al., 2012a; Zhu et al., 2012). In addition to the increase in anthropogenic emissions of aerosols and their precursors, climate change caused by anthropogenic and/or natural forcings also exerted great influence on the haze pollution in China, especially through changing the strength of the East Asian monsoon (Zhang et al., 2010, 2014b; Liu et al., 2011; Yan et al., 2011; Chin, 2012; Zhu et al., 2012; Mu and Zhang, 2014; Chen and Wang, 2015; Li et al., 2016a, b; Cai et al., 2017). Studies generally showed that the wintertime haze days across central and eastern China had a close negative relationship with the strength of the East Asian winter monsoon (EAWM; Zhang et al., 2014b; Mu and Zhang, 2014; Chen and Wang, 2015; Li et al., 2016a; Cai et al., 2017). In summer, the increase in surface aerosol concentration and optical depth over eastern and northern China correlated with the weakening of the East Asian summer monsoon (EASM; Zhang et al., 2010; Yan et al., 2011; Zhu et al., 2012), whereas Yang et al. (2014) found that the gaseous pollutant of surface O_3 over China had a positive relationship with the EASM.

Wang et al. (2015a) and Zou et al. (2017) revealed that the increasing winter haze pollution in eastern China in recent years was related to the decreasing Arctic sea ice in preceding autumn. Many studies suggested that under global warming, the future climate will be more stagnant and the weather conditions conducive to severe haze in eastern China will be more frequent (Jacob and Winner, 2009; Wang et al., 2015a; Cai et al., 2017). However, Jacob and Winner (2009) also pointed out that the effects of future climate change on particulate matter (PM) were complicated, as the projection of precipitation, wildfires, atmospheric chemistry, and natural emissions of aerosols by models is still in need of improvement.

El Niño–Southern Oscillation (ENSO) is the dominant changing mode of the tropical sea surface temperature (SST) on interannual scale (Rasmusson and Carpenter, 1982), of which the climatic effects are global (Bjerknes, 1972; Huang and Wu, 1989; Zhang et al., 1999; Lau and Nath, 2003; Zhai et al., 2016, etc.). ENSO influences not only the EASM (Chang et al., 2000; Li et al., 2007; Zhao et al., 2017, etc.) but also the EAWM, especially over low latitudes (Chen et al., 2013; He and Wang, 2013; Kim et al., 2016, etc.), which indicates that ENSO may affect the haze pollution over East Asia through influencing the monsoon circulation. Wu et al. (2013) found that the aerosol variations over the Maritime Continent and western North Pacific presented a biennial feature, which could be attributed to the impacts of ENSO. From the results of Wu et al. (2013), it seemed that ENSO only influenced the aerosols over eastern China (30–40° N, 110–120° E) around October in El Niño or La Niña developing years and July in El Niño or La Niña decaying years. Gao and Li (2015) revealed statistically and through case analyses that El Niño (La Niña) events were more likely to bring about more (fewer) haze days in eastern China (25–35° N, 105–122.5° E). Feng et al. (2016) simulated the influence of the 1994/1995 El Niño Modoki event on the aerosol concentrations over southern China (20–35° N, 105–120° E), and found that the aerosol concentrations increased during the mature phase (in boreal winter) of the event. Feng et al. (2017) simulated the influence of the 1998/1999 and 2000/2001 La Niña Modoki events on the aerosol concentrations over eastern China (105–120° E), and found that the geographical distributions of aerosols over eastern China during the winters of the two events were opposite with each other. Most previous studies discussed the effects of ENSO on the winter haze pollution of China based on observation or case simulation separately. In this study, we try to explore the effects of ENSO on the winter haze pollution of China statistically and numerically. ENSO is a recurring climate pattern, and many climate centers around the world monitor it systematically and use it in climate prediction extensively. Therefore, exploring the effects of ENSO on the winter haze pollution in China may provide useful information for the prediction of haze for the country.

The article is organized as follows: methodology is given in Sect. 2, including data and model introduction; results including statistical and model results are presented in Sect. 3, followed by conclusions and discussions in Sect. 4.

2 Methodology

2.1 Data used in statistical analysis

We first analyzed the relationship between the winter haze days of China and global SST in Sect. 3. The monthly haze days from the data set for haze project version 1.0 of the National Meteorological Information Center, China Meteorological Administration (CMA) were used. The CMA defines haze using visibility (< 10 km) and relative humidity (< 80 %; Tao et al., 2014). The time span of the data set is January 1954–July 2014, but only the data after 1960 were actually used in this study, as the data set has steadily included more than 2000 stations since 1960. A merged monthly SST data set (Hurrell et al., 2008) formed by the SST data of the Hadley Centre and the National Oceanic and Atmospheric Administration (NOAA) was used in the correlation analysis. The SST data together with a merged sea ice (SI) data set of the same sources were used in the following numerical simulation. The SST and SI data are both from 1870 to 2012, with a horizontal resolution of $1° \times 1°$.

2.2 Model description and experimental setup

The aerosol–climate coupled model BCC_AGCM2.0_CUACE/Aero (Zhang et al., 2012b) of the National Climate Center (NCC), CMA, was used in the numerical study of the effects of ENSO on atmospheric aerosol content. The coupled model comprises the NCC/CMA climate model (BCC_AGCM2.0; Wu et al., 2010) and the CMA Unified Atmospheric Chemistry Environment/Aerosol model (CUACE/Aero; Gong et al., 2002, 2003). The coupled model employs a horizontal T42 spectral resolution (about $2.8° \times 2.8°$) and a hybrid vertical coordinate with 26 levels, the top of which is located at about 2.9 hPa. Five types of aerosol (including emission, gaseous chemistry, transport, coagulation, and removal) are considered in the model: sulfate (SF), black carbon (BC), organic carbon (OC), dust, and sea salt. The emissions of the first three types of aerosol and/or their precursors are prescribed, and the last two types of aerosol are emitted online (Gong et al., 2002). The particle radii of each type of aerosol are divided into 12 size bins from 0.005 to 20.48 µm. Each type of aerosol is assumed to be externally mixed with the others. Sulfate, organic carbon, and sea salt are considered to be hygroscopic, and the other two types are

Table 1. Simulation setup.

Group name	SST	Running time	Output frequency
CLI	Climatologic SST	Oct^0–Aug^1	Monthly and daily
EL	Climatologic SST + $\Delta SST_{El\,Niño}$	Oct^0–Feb^1	Monthly and daily
LA	Climatologic SST + $\Delta SST_{La\,Niña}$	Oct^0–Feb^1	Monthly and daily

The superscripts of the third column of 0 and 1 represent the first and second model year, respectively.

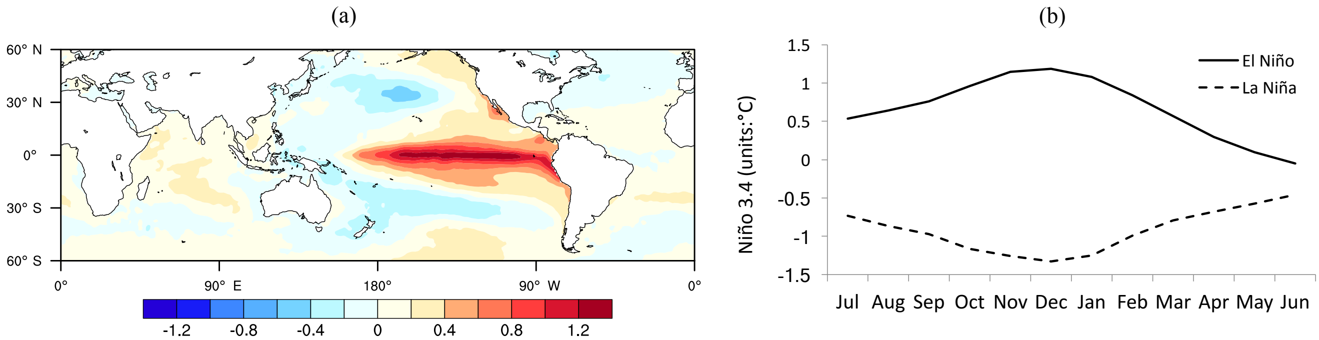

Figure 1. (a) Typical ENSO mode (units: °C/°C) and **(b)** average monthly Niño3.4 (units: °C) of 21 El Niño and 18 La Niña events from 1951 to 2015.

considered to be non-hygroscopic. The coupled model has been introduced, evaluated, and used in many studies of the radiative forcings and climatic effects of aerosols (e.g., Zhang et al., 2014a, 2016; Wang et al., 2015b; Zhao et al., 2014).

Three groups of experiments were conducted (Table 1), named CLI, EL, and LA (climatological means, El Niño and La Niña), with each group including 20 members by altering initial conditions. To get different initial conditions, a preparation experiment was run first with the model's default setting (Zhao et al., 2014). Three types of files (initial, restart, and history files) of the preparation experiment were output, and the output frequency was set to daily. Twenty initial files output from the preparation experiment were then used as the different initial conditions for different ensemble members. The group of CLI used the climatological mean (from 1981 to 2010) monthly SST and SI, which was introduced in Sect. 2.1 but interpolated to the model's resolution, as boundary conditions. In the groups of EL and LA, the climatological-mean monthly SST was superposed by El Niño and La Niña SST perturbations, respectively, and the SI was identical to that in CLI. The El Niño and La Niña SST perturbations were obtained by scaling a typical ENSO mode (Fig. 1a) with the average monthly Niño3.4 indices of 21 El Niño and 18 La Niña events (selected from 1951 to 2015, Fig. 1b), respectively. The Niño3.4 indices from January 1951 to the present can be downloaded from the website of NCC/CMA (cmdp.ncc-cma.net/download/Monitoring/Index/M_Oce_Er.txt). The typical ENSO mode was obtained through the regression between the monthly Niño3.4 index and the SST field after removing their linear trends. The running period of the group of CLI was from October to the following August, in order to confirm if the model can capture the general features of the circulations of the East Asian winter and summer monsoons. In the confirmation process, the geopotential height and wind from the National Centers for Environmental Prediction (NCEP) reanalysis data were used. The running periods of EL and LA were both from October to the following February. The results in boreal winter (December, January, and February: DJF) of the three groups were used in the analysis, using the two previous months for the atmosphere to respond to SST perturbations.

The emission data of SF, BC, OC, and/or their precursors used in all experiments were from the Representative Concentration Pathway 4.5 (RCP 4.5) of the Intergovernmental Panel on Climate Change (IPCC) for year 2010. In this study, only the changes in the atmospheric contents of SF, BC, and OC caused by different SST perturbations were analyzed, as the three types of aerosol were mainly emitted by anthropogenic activities and the important components of haze pollutants. In the analyzing process, the median instead of the average of the changes of a specific variable between different groups of experiments (e.g., EL–CLI) was used, as median is more robust and resistant to extreme large or small values that may happen in some ensemble members. In addition, we also marked the grids where the differences of a specific variable between more than 70 % of ensemble member pairs had the same sign as the median differences, as a reflection of significance.

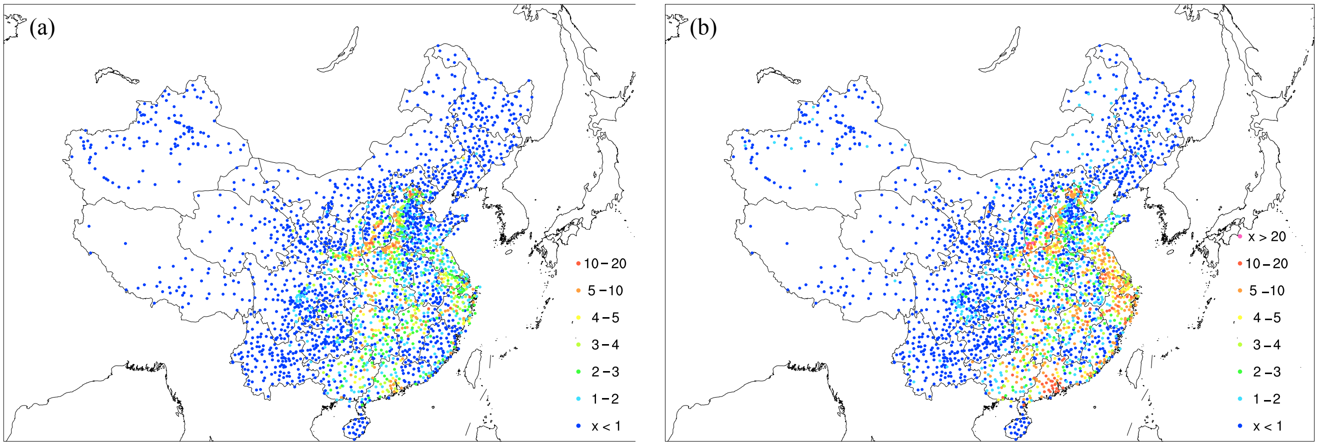

Figure 2. The winter-average monthly haze days (units: days month^{-1}) during years **(a)** 1960–2013 and **(b)** 2000–2013 over mainland China.

3 Results

3.1 Statistical results

In this section, we first present the geographical distribution of the winter haze days in mainland China over the past approximately 50 years and since year 2000. Then, three typical polluted regions are selected, and the correlations between their respective winter haze days and global SST are analyzed.

It can be seen from Fig. 2a that Beijing, southwestern Hebei, central and southern Shanxi, central Shaanxi, and northern Henan suffered from winter haze pollution more frequently than elsewhere in China during 1960–2013, with 10–20 days being the most common DJF mean monthly haze day ranges. The diffusive conditions of these areas are not good because of the influence of the Taihang and Qinling mountains. Besides the above areas, stations with more than 5–10 DJF mean monthly haze days during 1960–2013 were distributed densely in the provinces of Hubei, Hunan, Jiangxi, Zhejiang, Guangxi, and Guangdong. Compared with 1960–2013, winter haze pollution in mainland China generally became more frequent during 2000–2013 (Fig. 2b). For example, in the Yangtze River delta and Pearl River delta, there were many more stations with 5–10 and 10–20 DJF mean monthly haze days during 2000–2013 than during 1960–2013. At some stations of Shanxi Province, the DJF mean monthly haze days during 2000–2013 were even more than 20 (Fig. 2b). The locations of the Chinese provinces mentioned above and in the following can be found in Fig. S1 in the Supplement.

Three representative regions – JJJ (Beijing, Tianjin, and Hebei province; accounting for 179 stations), JZH (Jiangsu and Zhejiang provinces, and Shanghai; accounting for 164 stations), and GG (Guangdong and Guangxi provinces; accounting for 178 stations) – were selected to represent northern, eastern, and southern China, respectively. From

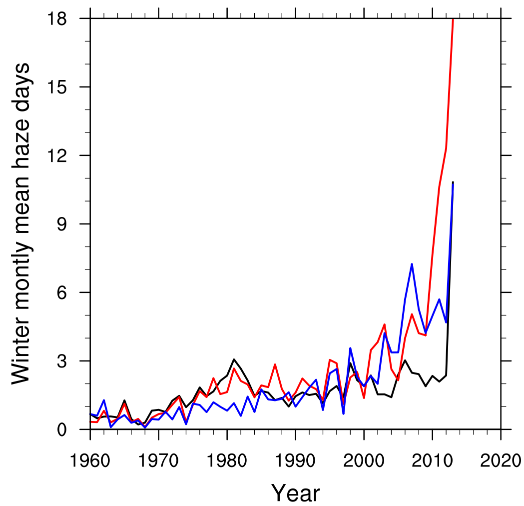

Figure 3. Time series of the winter-average monthly haze days (units: days month^{-1}) of JJJ (black), JZH (red), and GG (blue).

Fig. 3 we see that there were generally fewer than 3 DJF mean monthly haze days in these three regions before year 2000, with a small peak around 1980 in northern and eastern China. After year 2000, the number of DJF mean monthly haze days over eastern and southern China grew rapidly. The DJF mean monthly haze days of northern China increased much later than the other two regions after year 2000. Actually, the DJF mean monthly haze days over northern China were relatively few until 2012, which was consistent with the result of Chen and Wang (2015).

Considering that the increases in the DJF mean monthly haze days over eastern and southern China increased very abruptly after year 2010, only the winter haze days of the three regions from 1960 to 2010 were used in analyzing their relationships with winter SST. In order to remove the interdecadal variabilities, we applied 2–8-year band-pass filter-

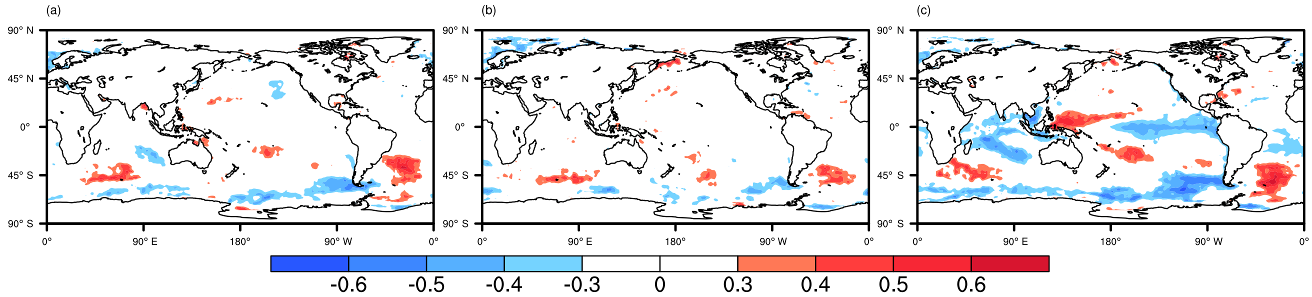

Figure 4. Correlation coefficients (unitless) of the monthly haze days of **(a)** JJJ, **(b)** JZH, and **(c)** GG with SST in winter, after applying band-pass filtering of 2–8 years to both the data of haze days and SST. Shade denotes that results pass 95 % significance level.

ing to both the data of haze days and SST. It can be seen from Fig. 4 that only the winter haze days of southern China had significant negative relationships with the equatorial SST over the central and eastern Pacific and central Indian Ocean, and positive relationships with the equatorial SST over the western Pacific. The geographical distribution of the correlation coefficients between the winter haze days over southern China and SST was generally an opposite phase of the typical ENSO mode shown in Fig. 1a, indicating that southern China tended to suffer from more (fewer) haze days than normal in La Niña (El Niño) winter. This could also be seen from the comparison of the DJF mean monthly haze days between several selected pairs of La Niña and El Niño winters over southern China (Fig. S2). In order to avoid the influence of the variations in the emissions of haze particles and their precursors, each pair of La Niña and El Niño winters were selected with intervals of no longer than 2 years.

The relationships between the winter haze days of northern and eastern China and equatorial SST were not significant (Fig. 4a and b), indicating that ENSO did not influence the winter haze days of these two regions significantly. This is probably because, as a tropical phenomenon, ENSO affects the climate over southern China more directly than over northern and eastern China, especially in winter when the western Pacific subtropical high (WPSH) is generally weaker and located further south than in other seasons. Zou et al. (2017) linked the extreme winter haze events over east China plains (112–122° E, 30–41° N, including JJJ and most parts of JZH) to Arctic sea ice loss in the preceding autumn and extensive Eurasia snowfall in early winter. Gao and Li (2015) found that the winter haze days of eastern China had positive relationship with the SST over the eastern equatorial Pacific. However, "eastern China" in Gao and Li (2015) included most regions between the Yangtze and Yellow rivers east of 105° E, which was much larger and further west than the representative region of eastern China in this work, and further south and west than the concerned region in Zou et al. (2017).

3.2 Model results

3.2.1 Winter and summer circulations, and atmospheric aerosol content

First, the simulated winter and summer circulations over East Asia in the group of CLI were checked by comparing with NCEP reanalysis data (Fig. 5). The model was able to capture the general features of the winter and summer circulations over East Asia. For example, in winter, the deepening of East Asian trough (EAT), the overwhelming of northwesterly over eastern China, and the strengthening of the easterly north of the Equator were all depicted by model results (Fig. 5a); in summer, the northward shift of WPSH and the strengthening of the cross-equatorial westerly over the Indian Ocean and Maritime Continent were also generally captured by the model (Fig. 5b). However, the EAT simulated by the model in winter was weaker and narrower, and located further west than NCEP reanalysis data. In summer, the simulated WPSH was weaker and located further east than NCEP reanalysis data. It seemed that the simulated cross-equatorial flow was stronger than reanalysis data both in winter and summer, which was probably the reason for the weakness of the simulated EAT in winter and WPSH in summer. In the model results of the group of CLI, the stronger cross-equatorial westerly over the Indian Ocean and Maritime Continent obstructed the westward stretch of the WPSH in summer, resulting in positive precipitation biases over South Asia and Southeast Asia, and negative precipitation biases over southern China (Zhao et al., 2014).

The simulated winter surface concentration (CONCsur) values and loadings of aerosols in the group of CLI (Fig. 6) showed that central and eastern China (east of about 105° E) were the most haze-polluted regions of the country, in line with the observational distribution of winter haze days shown in Fig. 2. The maximum of the winter CONCsur of aerosols was centered in Henan Province at about 20 $\mu g\,m^{-3}$. Compared with other observational studies (e.g., Cao et al., 2007; Zhang and Cao, 2015; Cai et al., 2017), the simulated CONCsur values of aerosols shown in Fig. 6a were underestimated by about 1–2 orders of magnitude. It should be noted

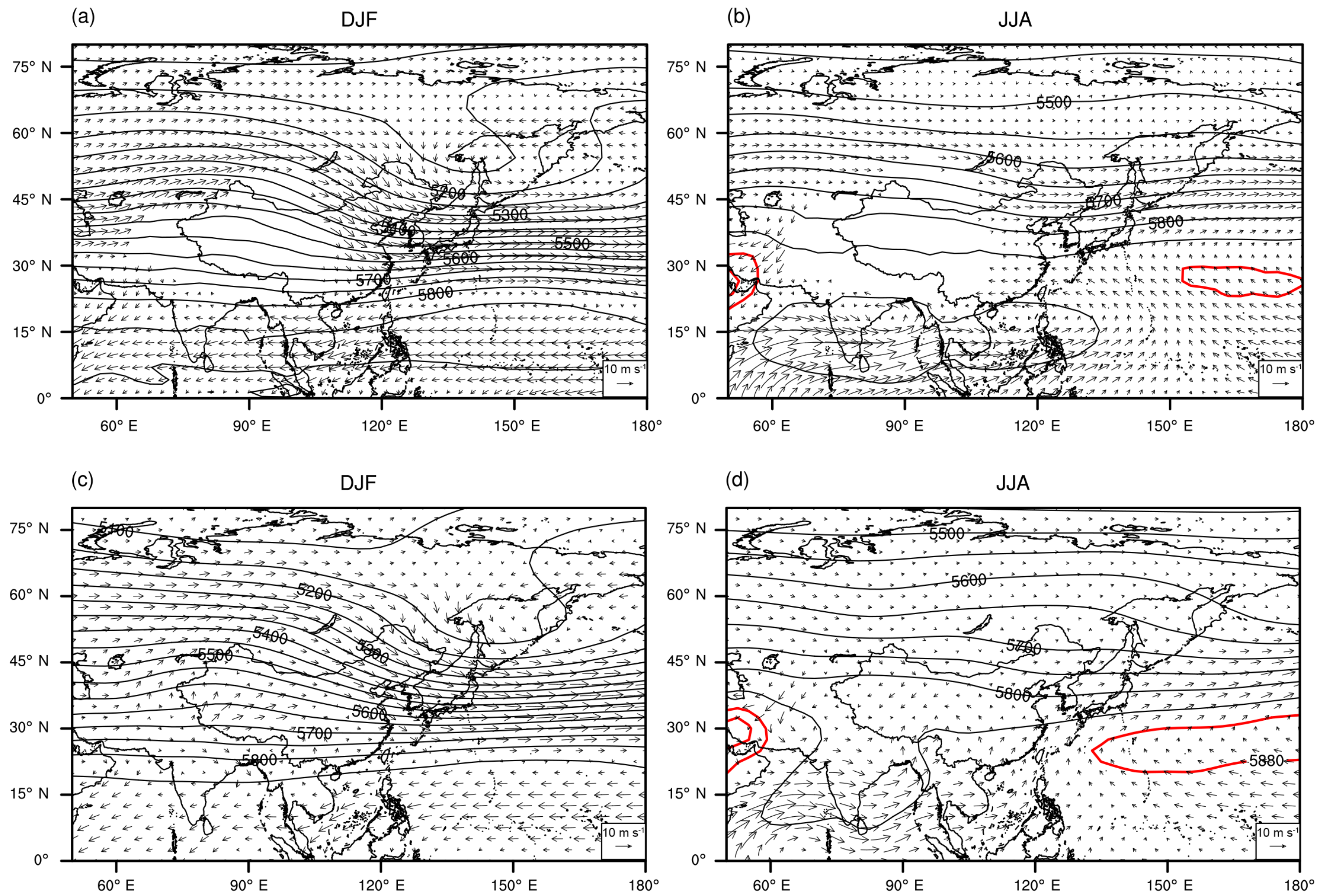

Figure 5. Comparisons between **(a, b)** the simulated and **(c, d)** reanalysis winter and summer geopotential height at 500 hPa (contour; units: geopotential meters, gpm) and wind at 850 hPa (vector; units: $m\,s^{-1}$), with the blank places in **(a)** and **(b)** are due to the influence of the Tibetan Plateau. Model results are from the group of CLI, and reanalysis data are from NCEP.

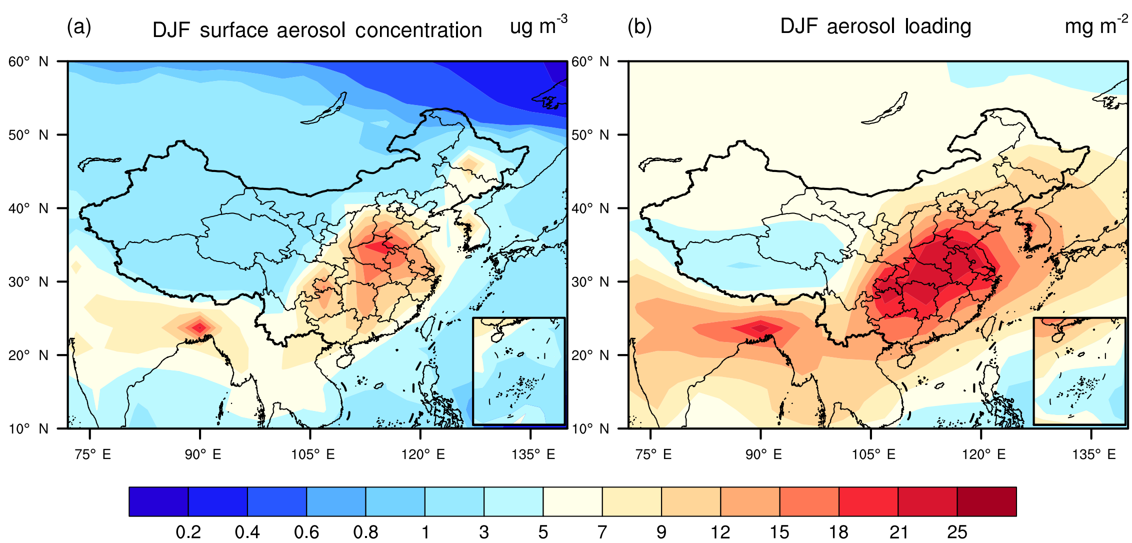

Figure 6. The simulated winter-average **(a)** surface aerosol concentrations (units: $\mu g\,m^{-3}$) and **(b)** aerosol loadings (units: $mg\,m^{-2}$) in the group of CLI.

that aerosol CONCsur values in this study were the lowest-level aerosol concentrations in the model. As introduced in Sect. 2.2, the model used in this study has 26 levels in the vertical hybrid σ–pressure axis, and the middle height of the lowest level is about 50–70 m above the surface in China (not shown). Therefore, the aerosol concentrations at the lowest level of the model actually reflect the mean of the aerosol concentrations from the surface to a height of about 100–140 m (or maybe even higher) above the surface. This certainly brought about underestimation as to aerosol CONCsur. Another reason for the underestimation was that we excluded all naturally emitted aerosols (dust and sea salt), in order to focus our attention on haze, as another meteorological phenomenon occurring frequently in late winter and spring over northern China – sandstorms – have quite different weather conditions than haze. The exclusion of naturally emitted aerosols was also the reason why the northwestern China was much cleaner than it was expected to be.

The maximum of the simulated winter aerosol loadings in China was 21–25 $mg\,m^{-2}$, and heavy aerosol loadings ($\geq 18\,mg\,m^{-2}$) in China were located east of 105° E, and between the Yellow and Yangtze rivers (Fig. 6b). The median of the 10 models that participated in the Aerosol Comparisons between Observations and Models (AeroCom; http://aerocom.met.no/cgi-bin/aerocom/surfobs_annualrs.pl) showed that the maximums of the loadings of SF, BC, and OC in January 2000 in China were 15–30, 2.5–5, and more than 10 $mg\,m^{-2}$, respectively. The model used in this study is also a member of AeroCom. Zhao et al. (2014) compared the simulated loadings of five kinds of aerosols (SF, BC, OC, sea salt, and dust) with the model using AeroCom median, and found that the model generally simulated the distributions and magnitudes of aerosol loadings well, though with some underestimations in BC and OC loadings.

3.2.2 The effects of ENSO on winter circulation and precipitation

The effects of ENSO on the winter circulation and precipitation over East Asia were discussed first, as these meteorological fields determine the transport, diffusion, and removal of aerosols, and consequently influence atmospheric aerosol content.

Two important features were apparent in the winter anomalous circulation field caused by El Niño (Fig. 7a). First, negative and positive anomalous geopotential heights at 500 hPa were seen near the Ural Mountains and Lake Baikal, respectively. Secondly, two anomalous anticyclones at 850 hPa were seen over the western North Pacific, with one in the Philippine Sea and the other one at the mid-latitudes. It was expected that the anomalous southwesterly in the northwest of the Philippine Sea anticyclone would bring more water vapor and also more aerosols to southern China, as Southeast Asia and South Asia were both areas with heavy aerosol loadings (Fig. 6b), whereas the anomalous geopotential heights at 500 hPa caused by La Niña were positive and negative near Ural Mountains and Lake Baikal, respectively, and two anomalous cyclones were caused by La Niña over the western North Pacific (Fig. 7b).

The differences in circulation between El Niño and La Niña winters were shown in Fig. 7c. It can be seen in Fig. 7c that the negative and positive anomalies in 500 hPa geopotential heights caused by El Niño were more obvious than that in Fig. 7a over the Ural Mountains and Lake Baikal, respectively. In addition, the anomalous anticyclones in the western North Pacific were also more obvious than that in Fig. 7a. Wang et al. (2000) found that the anomalous anticyclones over the western North Pacific formed in the boreal autumn of a developing El Niño, attained its peak in winter, and persisted into the following spring and early summer. In the sea level pressure field, the land–sea gradient in winter was decreased by El Niño (not shown), indicating that El Niño caused the weakness of the EAWM. The weakness of the EAWM caused by El Niño could also be seen from the weakness of East Asian jet stream and the decrease in EAWM index caused by El Niño (Fig. S3). The EAWM index used in Fig. S3 was the one defined by Li and Yang (2010). It has been suggested in previous studies that the weakness of East Asian jet stream and the Philippine Sea anticyclonic anomalies in winter caused by El Niño connected with each other by local Hadley circulation over East Asia (Kang and Lee, 2017).

Previous studies have also found that the EAWM tended to be weak in El Niño winter (e.g., Chen et al., 2000; Huang et al., 2012; Wang and Chen, 2014; Kang and Lee, 2017). Wang et al. (2000) has explored how ENSO influenced its upstream climate in East Asia and found that the Pacific–East Asian teleconnection (PEAT) was the key bridge. PEAT is a vorticity wave pattern that starts from the central Pacific and extends poleward and westward to East Asia. In Fig. 7c, PEAT could be recognized from the 850 hPa wind anomalies with a cyclonic vorticity over the central Pacific, the anticyclonic vorticities over the western North Pacific, and a cyclonic vorticity over northeast Asia. The PEAT could be seen more clearly from the differences in the stream function at 500 hPa between El Niño and La Niña winters (Fig. S4), which had the opposite sign of vorticity.

Corresponding to the anomalous anticyclones at 850 hPa over the western North Pacific caused by El Niño, winter precipitation decreased over Southeast Asia and the northwestern Pacific, and increased over southern China (Fig. 8a). In contrast, precipitation increased over Southeast Asia and the northwestern Pacific, and decreased over southern China during La Niña winter (Fig. 8b). The opposite effects of El Niño and La Niña on the winter precipitation over southern China can be seen more clearly in Fig. 8c, which was in accordance with the observational relationship between ENSO index and China precipitation in winter (http://cmdp.ncc-cma.net/pred/cn_enso.php?product=cn_enso_corr&season=DJF#corr). The decrease in

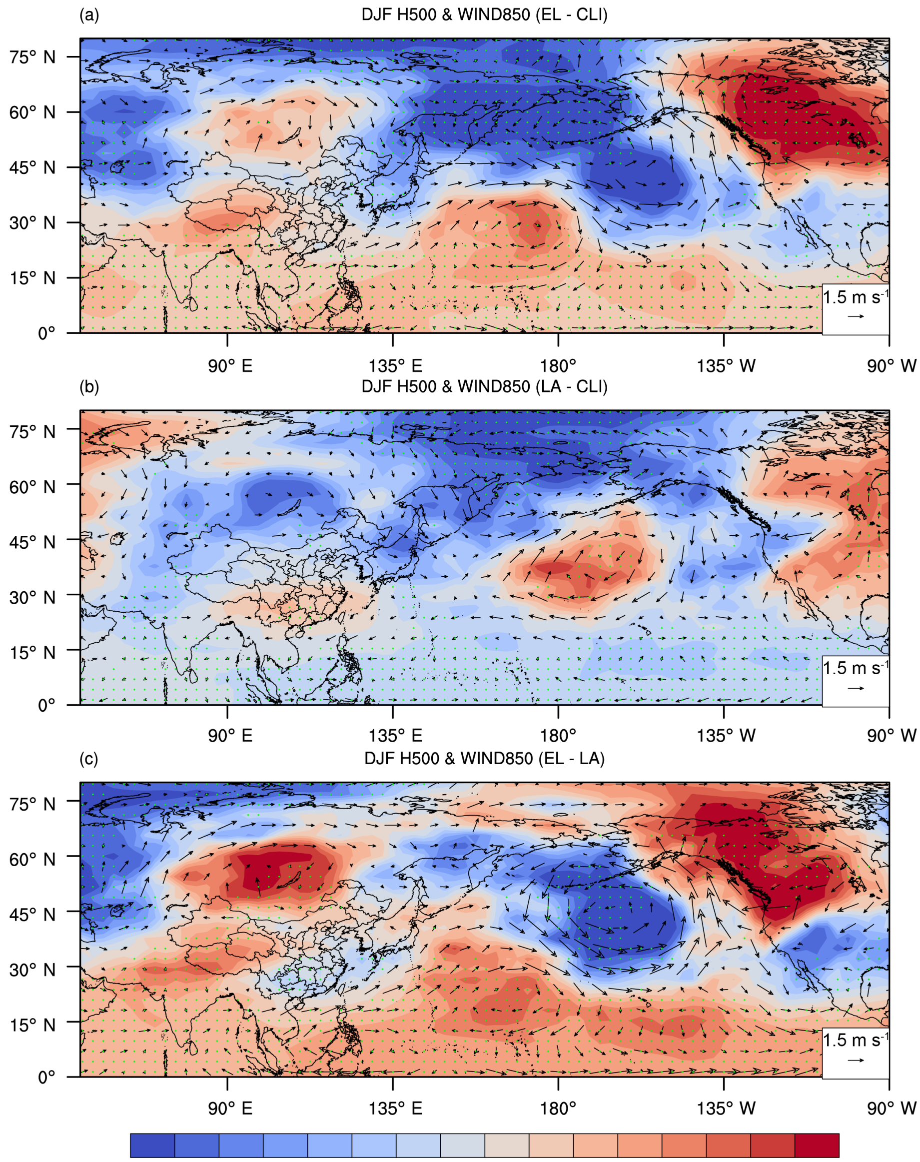

Figure 7. Medians of the simulated differences in winter-average geopotential height at 500 hPa (H500, shaded; units: gpm) and wind at 850 hPa (WIND850, vector; units: $m\,s^{-1}$) between **(a)** EL and CLI, **(b)** LA and CLI, and **(c)** EL and LA, with green dots indicating that the differences of H500 between more than 70 % of ensemble member pairs have the same sign as the median differences.

winter precipitation over southern China caused by La Niña was very likely the reason for the higher-than-normal number of haze days over the region during La Niña winter (Fig. 4c), as less precipitation meant slower cleaning of particles out of the atmosphere, which will be discussed in the next section (Fig. 11b and c). Another reason which should probably not be neglected is that drier conditions over southern China during La Niña winter could not allow for the confusion of haze days for fog days.

3.2.3 The effects of ENSO on winter atmospheric aerosol content

In this section, the changes in the winter aerosol CONCsur values and loadings over China caused by ENSO are presented, and then the mechanism by which ENSO affected winter atmospheric aerosol content is analyzed from the perspective of wet and dry depositions and interregional transport of aerosols.

It can be seen from Fig. 9a that the winter CONCsur values of aerosols were decreased by El Niño over northeastern China and eastern China. The winter aerosol CONCsur val-

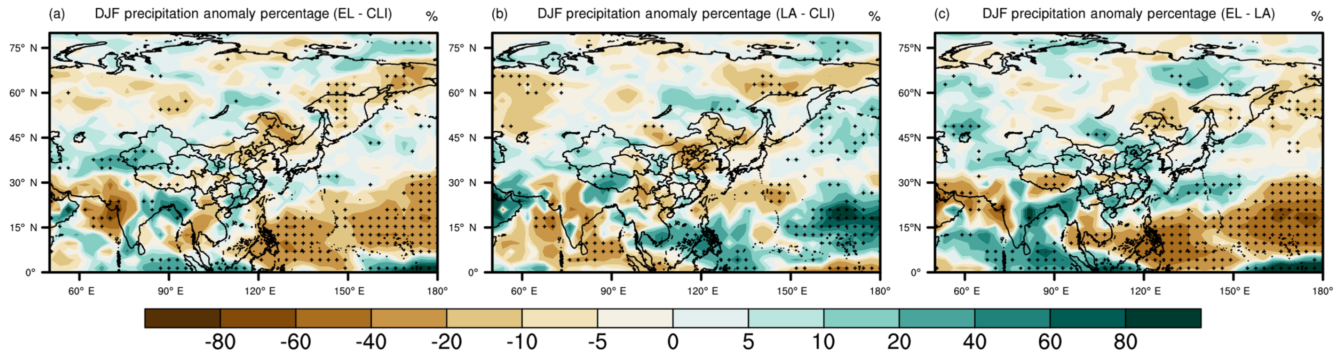

Figure 8. Medians of the simulated differences in winter-average precipitation in percentage (%) between **(a)** EL and CLI, **(b)** LA and CLI, and **(c)** EL and LA, with black dots indicating that the differences between more than 70 % of ensemble member pairs have the same sign as the median differences.

ues were also decreased by La Niña over northeastern China and eastern China, as well as part of northern China and most areas south of the Yangtze River (Fig. 9b). Over southern China, although the increases in the winter CONCsur values of aerosols caused by El Niño were not very clear in Fig. 9a, they were obvious by comparing with La Niña winter (Fig. 9c), which was generally in line with the simulation result of Feng et al. (2016). It can be seen in Fig. 9d that the winter aerosol loadings were increased by El Niño over most areas east of 105° E and south of 40° N, and decreased over northeastern China and part of northern China. In Fig. 9e, it can be seen that the anomalous winter aerosol loadings caused by La Niña presented a meridional "− + −" pattern over eastern China. The different influences of El Niño and La Niña on the winter aerosol loadings were the most obvious over large areas south of the Yangtze River (Fig. 9f).

From Fig. 9c and f, it was found that the differences in atmospheric aerosol content between El Niño and La Niña winters were more obvious over southern China than other areas of the country. To obtain more information, Fig. 9c and f were plotted in another way with different significance levels (Fig. S5), which also showed that ENSO affected winter atmospheric aerosol content over southern China more obviously than it did over other areas of the country. This was to some extent in line with the results in Fig. 4 that only the winter haze days over southern China had significant relationship with ENSO. Therefore, in the following analysis, we focused on the mechanism how ENSO affected winter atmospheric aerosol content over southern China.

In Sect. 3.1, we discussed that the haze days over southern China tended to be fewer (more) than normal in El Niño (La Niña) winter, which was to some extent contradictory to the increase (decrease) in winter atmospheric aerosol content over southern China caused by El Niño (La Niña). In the following, we first explain why the changes in the winter haze days and atmospheric aerosol content caused by ENSO over southern China were not consistent with each other. Then, we explore the reasons for the increase (decrease) in winter atmospheric aerosol content caused by El Niño (La Niña) over southern China.

Figure 4c showed statistically that southern China tended to suffer from more (fewer) haze days than normal in La Niña (El Niño) winter, which was also seen in the four selected pairs of El Niño and La Niña winters (Fig. S2) with one of them near 2010 (in numerical simulations, the aerosol emissions were fixed in 2010). However, numerical results showed that La Niña (El Niño) caused a decrease (increase) in winter atmospheric aerosol content over southern China (Fig. 9). Is it possible for southern China to have more (fewer) haze days but less (greater) atmospheric aerosol content than normal in La Niña (El Niño) winter? To answer this question, the frequency distributions of the simulated winter daily aerosol CONCsur values averaged over southern China (21–27° N, 104–118° E; see Fig. S1) in the groups of CLI, EL, and LA were plotted in Fig. 10. Section 3.2.1 demonstrated that the simulated aerosol CONCsur values in this study were smaller than observational studies by 1–2 orders of magnitude. Therefore, for calibration, the simulated winter daily aerosol CONCsur values over southern China were amplified by 10 before plotting the frequency distributions.

It can be seen from Fig. 10 that the frequency distribution of the simulated winter daily aerosol CONCsur over southern China was a little right-skewed in the group of CLI, reaching peak at around 65 $\mu g\, m^{-3}$. The frequency distribution of the simulated winter daily aerosol CONCsur over southern China in the group of LA was a little left-shifting compared with that in CLI when aerosol CONCsur was larger than 40 $\mu g\, m^{-3}$. The frequency distribution of the simulated winter daily aerosol CONCsur over southern China in EL was a little right-shifting compared with that in CLI. The average numbers of days in winter with aerosol CONCsur values below 40, between 40 and 80, and above 80 $\mu g\, m^{-3}$ in CLI, EL, and LA were also given in the top right corner of Fig. 10. It was found that the number of days in winter with aerosol CONCsur values between 40 and 80 $\mu g\, m^{-3}$ was the largest in LA and smallest in EL, whereas the number of days in

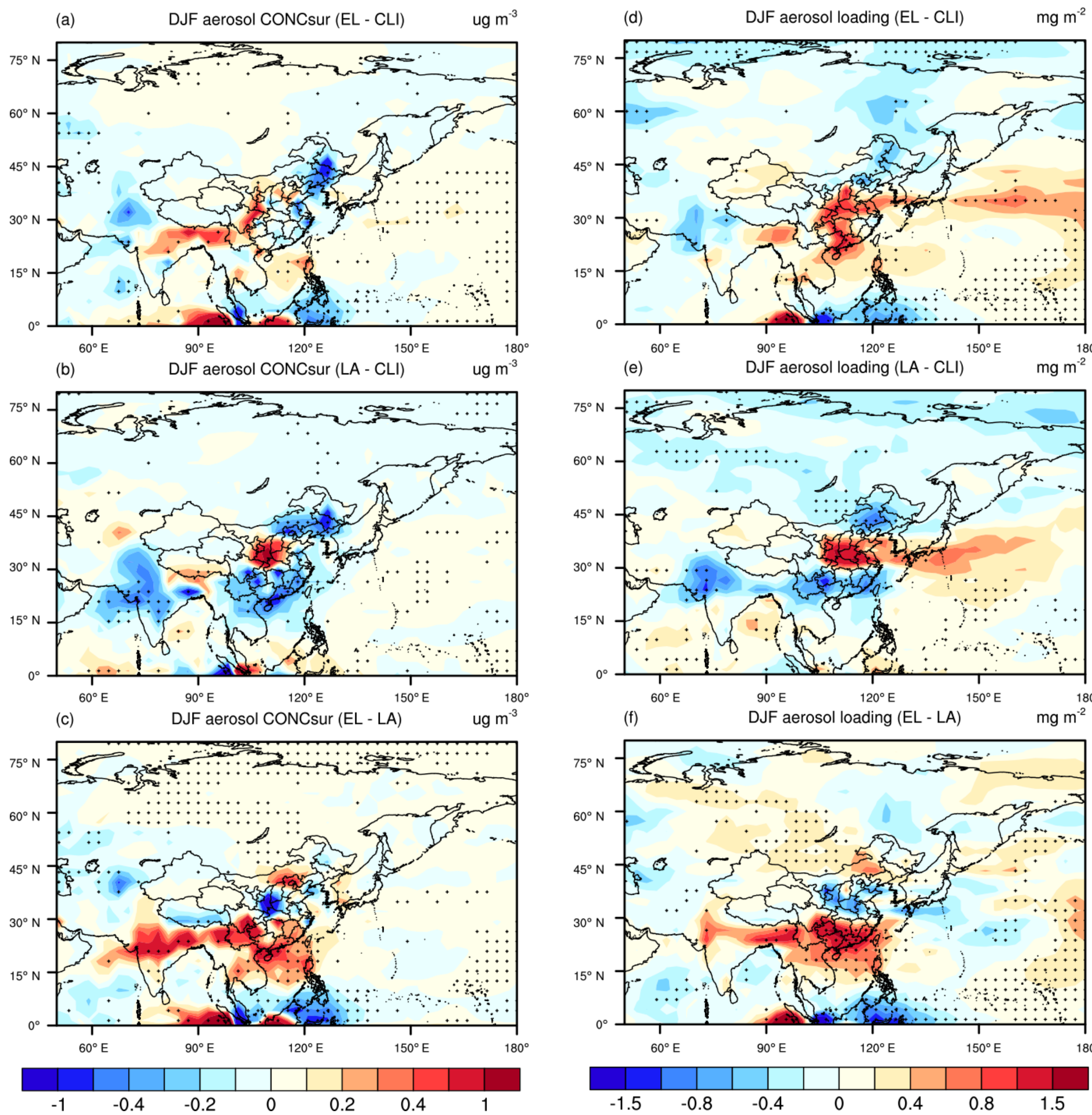

Figure 9. Medians of the simulated differences in winter-average aerosol surface concentrations (left panel; units: $\mu g\,m^{-3}$) and aerosol loadings (right panel; units: $mg\,m^{-2}$) between EL and CLI **(a, d)**, LA and CLI **(b, e)**, and EL and LA **(c, f)**, with black dots indicating that the differences between more than 70 % of ensemble member pairs have the same sign as the median differences.

winter with aerosol CONCsur values above $80\,\mu g\,m^{-3}$ was the largest in EL and smallest in LA. Figure 10 indicated that southern China tended to have a smaller number of clean and heavy haze days but a greater number of moderate haze days than normal in La Niña winter, whereas in El Niño winter, southern China tended to have a greater number of heavy haze days but fewer clean and moderate haze days than normal. This explained why southern China had fewer (more) haze days but greater (less) atmospheric aerosol content than normal in El Niño (La Niña) winter. It should be noted that here we used regional mean aerosol CONCsur values over southern China subjected to the low model spatial resolution, which was the reason why the curves in Fig. 10 were close to each other. In practice, however, haze days and their severities are judged station by station (e.g., Fig. 2), and the thresholds are not necessarily the same as those used in Fig. 10. Therefore, we can get some rough information about the effects of ENSO on the winter haze days over southern China from the shifts of curves in Fig. 10, but cannot compare it with observational data directly.

As the emissions of aerosols were kept the same in all experiments (Sect. 2.2), the speed at which aerosols were removed from the atmosphere, especially through wet deposition, could affect atmospheric aerosol content greatly (Zhang et al., 2016). It was found that ENSO influenced the winter wet depositions more obviously than the winter dry deposi-

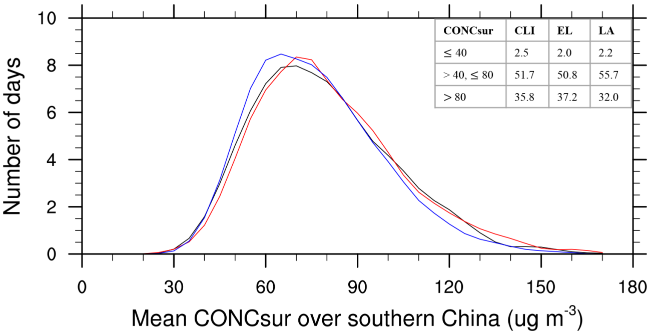

Figure 10. Frequency distributions of the simulated winter daily surface aerosol concentrations (CONCsur; units: $\mu g\,m^{-3}$) averaged over southern China (after being amplified by 10), with black, red, and blue lines representing the results from CLI, EL, and LA, respectively. The average numbers of days in winter with CONCsur ≤ 40, $40 <$ CONCsur ≤ 80, and CONCsur > 80 in CLI, EL, and LA are given in the table at the top right corner.

tions of aerosols over China (Fig. 11). The winter dry depositions of aerosols were decreased both by El Niño and La Niña over southern China (Fig. 11c–f). Compared with dry deposition, wet deposition is a faster process. The winter wet depositions of aerosols over southern China were increased (decreased) by El Niño (La Niña; Fig. 11a–c), corresponding to the changes in winter precipitation (Fig. 8). Comparing Figs. 9 and 11, it was found that the winter atmospheric contents and wet depositions of aerosols were both increased (decreased) by El Niño (La Niña) over southern China. It seemed that the changes in the winter wet depositions of aerosols were the result rather than the reason for the changes in winter atmospheric aerosol content over southern China.

Besides local emission and removal, the interregional transport of aerosols could also influence atmospheric aerosol content over a specific region. It was mentioned in Zhang et al. (2016) that South and Southeast Asia had become important source areas of anthropogenic aerosols in 2010, which was also seen in the simulated aerosol CONCsur values and loadings over these regions (Fig. 6). A low-level anomalous anticyclone (cyclone) was caused by El Niño (La Niña) over the Philippine Sea in winter (Fig. 7). The southwesterly (northeasterly) at the northwest of the anomalous anticyclone (cyclone) led to enhanced (weakened) transport of aerosols from South and Southeast Asia to southern China in El Niño (La Niña) winter (Fig. 12). As the changes in winter atmospheric aerosol content over southern China caused by ENSO could not be explained by local emission or removal, it could only be attributed to the changes in the transport of aerosols from South and Southeast Asia to southern China. Zhu et al. (2012) has also pointed out that in determining aerosol concentrations, the changes in monsoon circulation were more dominant than that in precipitation (or wet deposition of particles) in East Asia. It is expected that when the emissions of aerosols over South and Southeast Asia diminish in the future, the contradiction between the influence of ENSO on winter haze days and on atmospheric aerosol content over southern China will also disappear.

4 Conclusions and discussions

The effects of ENSO on winter haze days and atmospheric aerosol content over China were discussed statistically and numerically. Statistical results showed that southern China tended to have fewer (more) haze days than normal in El Niño (La Niña) winter, which was in line with the simulated greater (less) winter precipitation over southern China caused by El Niño (La Niña). Statistical results indicated that the relationships between the winter haze days over northern and eastern China and ENSO were not significant. Numerical results also revealed that the influence of ENSO on winter atmospheric aerosol content over northern and eastern China was not as obvious as over southern China. As a tropical phenomenon, it seemed that ENSO affected the winter haze pollution over southern China more significantly than it did over northern and eastern China.

Numerical results indicated that atmospheric aerosol content over southern China was greater (less) than normal in El Niño (La Niña) winter, which was to some extent not in line with the effects of ENSO on the winter haze days of the region. In 2010, South and Southeast Asia became important source areas of anthropogenic aerosols (Zhang et al., 2016). The enhanced southwesterly (northeasterly) at the northwest of the winter anomalous anticyclone (cyclone) over the Philippine Sea caused by El Niño (La Niña) enhanced (weakened) the transport of aerosols from South and Southeast Asia to southern China. The frequency distributions of the simulated daily surface concentrations of aerosols in winter over southern China indicated that the region tended to have a greater number of heavy (moderate) haze days, but fewer clean and moderate (heavy) haze days than normal in El Niño (La Niña) winter. However, it should be noted again that the emission data of aerosols used in our study were fixed in 2010, and if the emissions of aerosols change the effects may be different.

Many studies have found that the haze pollution over northern and eastern China was influenced by the EAWM, as cited in Sect. 1. In addition, previous studies also found that ENSO could influence the strength of the EAWM, as discussed in Sect. 3.2.2 that El Niño could weaken the EAWM. It was expected that there would be some connection between ENSO and the winter haze pollution over northern and eastern China. However, the connection between ENSO and the winter haze pollution over northern and eastern China was not strong; i.e., the correlations between the winter haze days of the two regions and ENSO were not significant. This made us consider how haze pollutants over northern China were cleared away in winter. Usually, a few clean days in

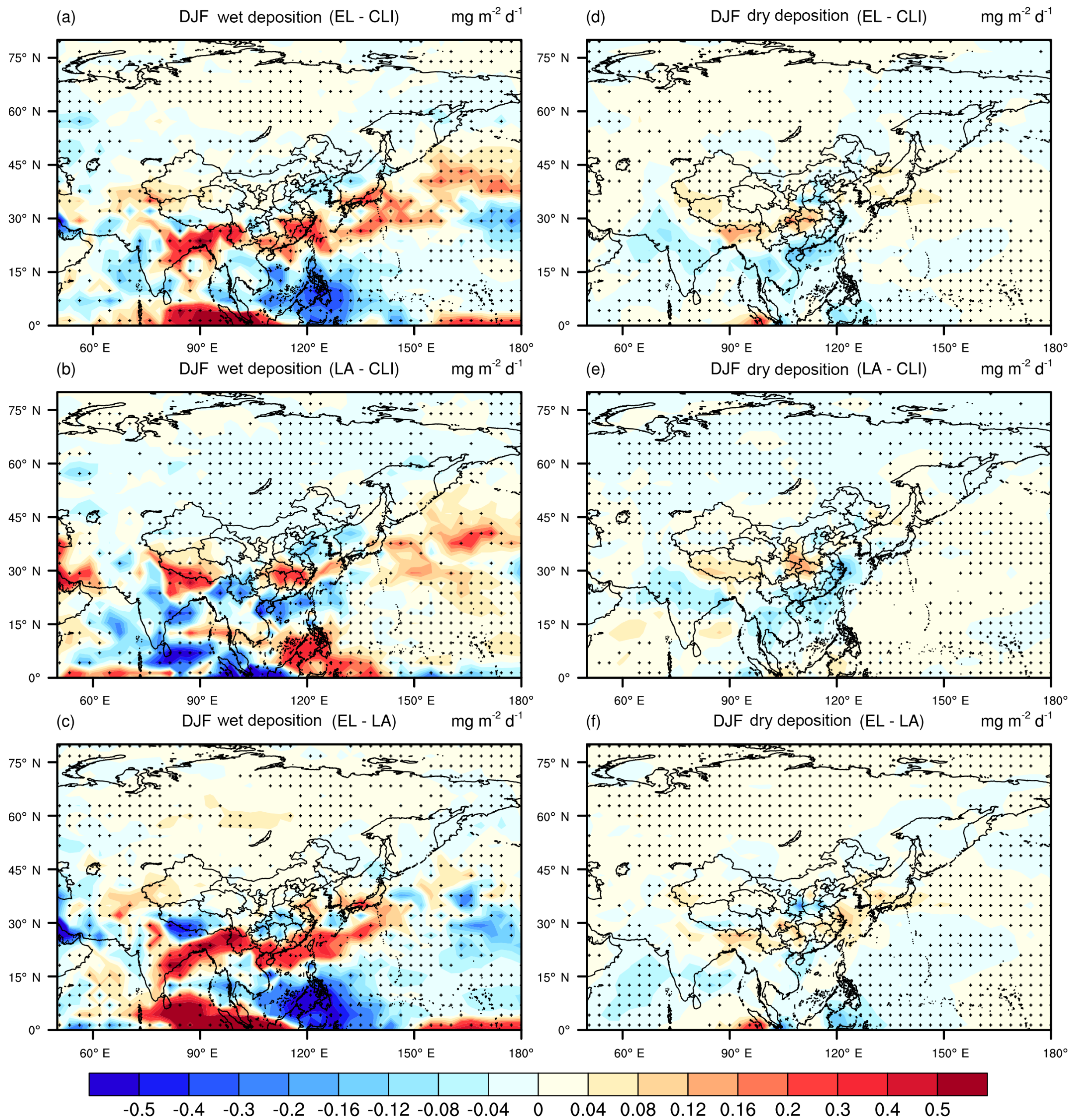

Figure 11. Medians of the simulated differences in winter-average wet depositions (left panel) and dry depositions (right panel) of aerosols (units: $mg\,m^{-2}\,d^{-1}$) between EL and CLI **(a, d)**, LA and CLI **(b, e)**, and EL and LA **(c, f)**, with black dots indicating that the differences between more than 70 % of ensemble member pairs have the same sign as the median differences.

northern China followed a breakout of an atmospheric blocking over high-latitude Asia, during which a stream of cold air swept southwardly and rapidly from Siberia or Mongolia. Therefore, we obtained some information about the influence of ENSO on the winter haze pollution over northern China from the frequency of cold air recorded in China in El Niño and La Niña winters. In both December 1986 (during the 1986/1987 El Niño event) and December 2010 (during the 2010/2011 La Niña event), cold air appeared in China 7 times, equaling the maximum frequency of cold air days in December during 1960–2011 (Fig. S6). This indicated that El Niño (La Niña) did not necessarily reduce (increase) the cold air frequency of China in winter, even though it could weaken (strengthen) the EAWM. To the contrary, it seemed that El Niño (La Niña) conditions were favorable for (not favorable for) the appearance of cold air in China in winter (Fig. S7). The relationship between ENSO and the cold air frequency of China in winter made the connection be-

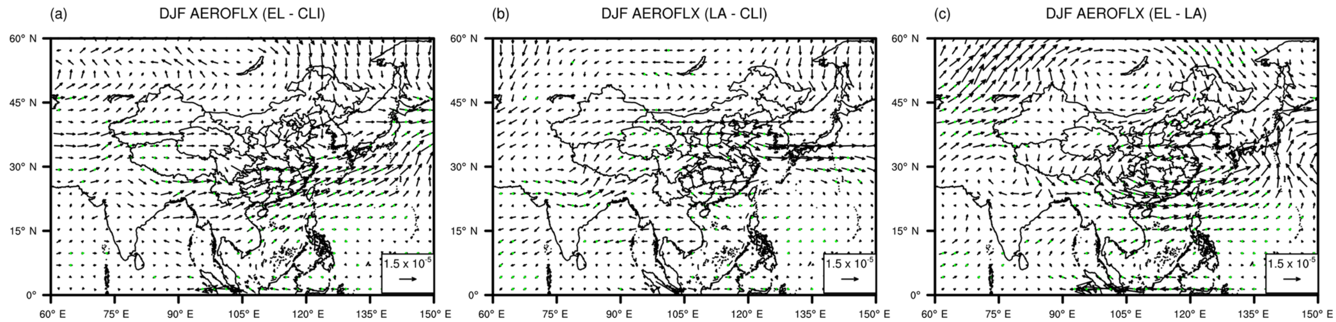

Figure 12. Medians of the simulated differences in the winter-average vertical integral of aerosol horizontal fluxes (AEROFLX; units: $kg\,m^{-1}\,s^{-1}$) between **(a)** EL and CLI, **(b)** LA and CLI, and **(c)** EL and LA, with green dots indicating that the differences of the zonal components of AEROFLX between more than 70 % of ensemble member pairs have the same sign as the median differences.

tween ENSO and the winter haze pollution over the northern China more complicated than expected simply from the perspective of the EAWM. The cold air frequency of China in winter is also influenced by the upstream conditions in the Atlantic Ocean, the Arctic ice, and the Eurasian snow cover (not shown). This emphasizes the importance of exploring the comprehensive effects of ENSO and the extratropical systems on the haze pollution of China.

Haze pollution is a very sophisticated problem because it is the comprehensive result of human activities and weather conditions. Weather conditions determine the dispersion and removal of haze particles over a specific region, influence the complex chemistry reactions among different components, and also connect the haze pollution of a specific region with the emissions of neighboring regions. Complicating matters further, haze pollution and weather conditions interact with each other closely over some areas. This work explores the effects of ENSO on the winter haze pollution over China under relatively simple experimental settings, with prescribed SST and fixed aerosol emissions, which means that SST does not response to aerosols. Additionally, the chemistry reactions in the model we used are also simplified, especially without the complex reactions related to nitrate aerosols. Therefore, studies with more sophisticated experimental designs (e.g., with atmosphere–ocean coupled models) and chemistry schemes are still needed for related future research on this topic.

Data availability. The data set for haze project version 1.0 of the National Meteorological Information Center, China Meteorological Administration, is not yet available for the public to download. The merged SST and SI data set of the Hadley Centre and the National Oceanic and Atmospheric Administration is available at https://climatedataguide.ucar.edu/climate-data/. The National Centers for Environmental Prediction (NCEP) reanalysis data are available at ftp://ftp.cdc.noaa.gov/Datasets//ncep.reanalysis/surface. Model simulation results are available at http://doi.org/10.5281/zenodo.1167952.

The Supplement related to this article is available online at https://doi.org/10.5194/acp-18-1863-2018-supplement.

Author contributions. The work was done under the guidance of Hua Zhang. Shuyun Zhao and Hua Zhang designed the experiment and prepared the manuscript. Bing Xie conducted model simulations. The analysis of results and preparation of all figures and tables were done by Shuyun Zhao.

Competing interests. The authors declare that they have no conflict of interest.

Acknowledgements. This work was financially supported by the (Key) National Natural Science Foundation of China (91644211 & 41575002). In addition, we would like to thank Shao Sun of the National Climate Center, Chinese Meteorological Administration, for his kind help in plotting figures.

Edited by: Toshihiko Takemura
Reviewed by: three anonymous referees

References

Bjerknes, J.: Large-scale atmospheric response to the 1964–65 Pacific equatorial warming, J. Phys. Oceanogr., 2, 212–217, https://doi.org/10.1175/1520-0485(1972)002<0212:LSARTT>2.0.CO;2, 1972.

Cai, W.-J., Li, K., Liao, H., Wang, H.-J., and Wu, L.-X.: Weather conditions conducive to Beijing severe haze more frequent under climate change, Nat. Clim. Change, 7, 257–262, https://doi.org/10.1038/nclimate3249, 2017.

Cao, J.-J., Lee, S.-C., Chow, J.-C., Watson, J. G., Ho, K.-F., Zhang, R.-J., Jin, Z.-D., Shen, Z.-X., Chen, G.-C., Kang, Y.-M., Zou, S.-C., Zhang, L.-Z., Qi, S.-H., Dai, M.-H., Cheng, Y., and Hu, K.: Spatial and seasonal distributions of carbonaceous aerosols over China, J. Geophys. Res., 112, D22S11, https://doi.org/10.1029/2006JD008205, 2007.

Chang, C.-P., Zhang, Y.-S., and Li, T.: Interannual and interdecadal variations of the East Asian summer monsoon and tropical Pacific SSTs. Part I: Roles of the subtropical ridge, J. Climate, 13, 4310–4325, https://doi.org/10.1175/1520-0442(2000)013<4310:IAIVOT>2.0.CO;2, 2000.

Chen, H.-P. and Wang, H.-J.: Haze days in North China and the associated atmospheric circulations based on daily visibility data from 1960 to 2012, J. Geophys. Res.-Atmos., 120, 5895–5909, https://doi.org/10.1002/2015JD023225, 2015.

Chen, W., Graf, H. F., and Huang, R.-H.: The interannual variability of East Asian winter monsoon and its relation to the summer monsoon, Adv. Atmos. Sci., 17, 48–60, https://doi.org/10.1007/s00376-000-0042-5, 2000.

Chen, W., Lan, X.-Q., Wang, L., and Ma, Y.: The combined effects of the ENSO and the Arctic Oscillation on the winter climate anomalies in East Asia, Chinese Sci. Bull., 58, 1355–1362, https://doi.org/10.1007/s11434-012-5654-5, 2013.

Chin, M.: Dirtier air from a weaker monsoon, Nat. Geosci., 5, 449–450, https://doi.org/10.1038/ngeo1513, 2012.

Dawson, J. P., Adams, P. J., and Pandis, S. N.: Sensitivity of $PM_{2.5}$ to climate in the Eastern US: a modeling case study, Atmos. Chem. Phys., 7, 4295–4309, https://doi.org/10.5194/acp-7-4295-2007, 2007.

Ding, Y.-H. and Liu, Y.-J.: Analysis of long-term variations of fog and haze in China in recent 50 years and their relations with atmospheric humidity, Sci. China Earth Sci., 57, 36–46, https://doi.org/10.1007/s11430-013-4792-1, 2014.

Feng, J., Li, J.-P., Zhu, J.-L., and Liao, H.: Influences of El Nino Modoki event 1994/1995 on aerosol concentrations over southern China, J. Geophys. Res.- Atmos., 121, 1637–1651, https://doi.org/10.1002/2015JD023659, 2016.

Feng, J., Li, J.-P., Zhu, J.-L., Liao, H., and Yang, Y.: Simulated contrasting influences of two La Niña Modoki events on aerosol concentrations over eastern China, J. Geophys. Res.- Atmos., 122, 2734–2749, https://doi.org/10.1002/2016JD026175, 2017.

Gao, H. and Li, X.: Influences of El Nino Southern Oscillation events on haze frequency in eastern China during boreal winters, Int. J. Climatol., 35, 2682–2688, https://doi.org/10.1002/joc.4133, 2015.

Gong, S.-L., Barrie, L. A., and Lazare, M.: Canadian Aerosol Module (CAM): a size-segregated simulation of atmospheric aerosol processes for climate and air quality models 2. Global sea-salt aerosol and its budgets, J. Geophys. Res., 107, D244779, https://doi.org/10.1029/2001JD002004, 2002.

Gong, S.-L., Barrie, L. A., Blanchet, J.-P., von Salzen, K., Lohmann, U., Lesins, G., Spacek, L., Zhang, L.-M., Girard, E., Lin, H., Leaitch, R., Leighton, H., Chylek, P., and Huang, P.: Canadian aerosol module: a size-segregated simulation of atmospheric aerosol processes for climate and air quality models 1. Module development, J. Geophys. Res., 108, D14007, https://doi.org/10.1029/2001JD002002, 2003.

He, S.-P. and Wang, H.-J.: Oscillating relationship between the East Asia winter monsoon and ENSO, J. Climate, 26, 9819–9838, https://doi.org/10.1175/JCLI-D-13-00174.1, 2013.

Huang, R.-H. and Wu, Y.-F.: The influence of ENSO on the summer climate change in China and its mechanism, Adv. Atmos. Sci., 6, 21–32, https://doi.org/10.1007/BF02656915, 1989.

Huang, R.-H., Chen, J.-L., Wang, L., and Lin, Z.-D.: Characteristics, processes, and causes of the spatio-temporal variabilities of the East Asian monsoon system, Adv. Atmos. Sci., 29, 910–942, https://doi.org/10.1007/s00376-012-2015-x, 2012.

Hurrell, J. W., Hack, J. J., Shea, D., Caron, J. M., and Rosinski, J.: A new sea surface temperature and sea ice boundary data set for the Community Atmosphere Model, J. Climate, 21, 5145–5153, https://doi.org/10.1175/2008JCLI2292.1, 2008.

Jacob, D. J. and Winner, D. A.: Effects of climate change on air quality, Atmos. Environ., 43, 51–63, https://doi.org/10.1016/j.atmosenv.2008.09.051, 2009.

Kang, D. and Lee, M.-I.: ENSO influence on the dynamical seasonal prediction of the East Asian Winter Monsoon, Clim. Dynam., https://doi.org/10.1007/s00382-017-3574-4, 2017.

Kim, J.-W., An, S.-I., Jun, S.-Y., Park, H.-J., and Yeh, S.-W.: ENSO and East Asian Winter Monsoon relationship modulation associated with the anomalous northwest Pacific anticyclone, Clim. Dynam., 4, 1157–1179, https://doi.org/10.1007/s00382-016-3371-5, 2016.

Lau, N.-C. and Nath, M. J.: Atmosphere–ocean variations in the Indo–Pacific sector during ENSO episodes, J. Climate, 16, 3–20, https://doi.org/10.1175/1520-0442(2003)016<0003:AOVITI>2.0.CO;2, 2003.

Li, Y. and Yang, S.: A dynamical index for the East Asian Winter Monsoon, J. Climate, 23, 4255–4262, https://doi.org/10.1175/2010JCLI3375.1, 2010.

Li, Y., Lu, R.-Y., and Dong, B.-W.: The ENSO–Asian monsoon interaction in a coupled ocean–atmosphere GCM, J. Climate, 20, 5164–5177, https://doi.org/10.1175/JCLI4289.1, 2007.

Li, Q., Zhang, R.-H., and Wang, Y.: Interannual variation of the wintertime fog-haze days across central and eastern China and its relation with East Asian Winter Monsoon, Int. J. Climatol., 36, 346–354, https://doi.org/10.1002/joc.4350, 2016a.

Li, Z.-Q., Lau, W. K.-M., Ramanathan, V., Wu, G., Ding, Y., Manoj, M.-G., Liu, J., Qian, Y., Li, J., Zhou, T., Fan, J., Rosenfeld, D., Ming, Y., Wang, Y., Huang, J., Wang, B., Xu, X., Lee, S.-S., Cribb, M., Zhang, F., Yang, X., Zhao, C., Takemura, T., Wang, K., Xia, X., Yin, Y., Zhang, H., Guo, J., Zhai, P.-M., Sugimoto, N., Babu, S.-S., and Brasseur, G.-P.: Aerosol and monsoon climate interactions over Asia, Rev. Geophys., 54, 866–929, https://doi.org/10.1002/2015RG000500, 2016b.

Liu, X.-D., Yan, L.-B., Yang, P., Yin, Z.-Y., and North, G. R.: Influence of Indian Summer Monsoon on aerosol loading in East Asia, J. Appl. Meteorol. Clim., 50, 523–533, https://doi.org/10.1175/2010JAMC2414.1, 2011.

Mu, M. and Zhang, R.-H.: Addressing the issue of fog and haze: a promising perspective from meteorological science and technology, Sci. China Earth Sci., 57, 1–2, https://doi.org/10.1007/s11430-013-4791-2, 2014.

Rasmusson, E. M. and Carpenter, T. H.: Variations in tropical sea surface temperature and surface wind fields associated with the Southern Oscillation/El Niño, Mon. Weather Rev., 110, 354–384, https://doi.org/10.1175/1520-0493(1982)110<0354:VITSST>2.0.CO;2, 1982.

Tao, M.-H., Chen, L.-F., Xiong, X.-Z., Zhang, M.-G., Ma, P.-F., Tao, J.-H., and Wang, Z.-F.: Formation process of the widespread extreme haze pollution over northern China in January 2013: implications for regional air quality and climate, Atmos. Environ., 98, 417–425, https://doi.org/10.1016/j.atmosenv.2014.09.026, 2014.

Tao, M.-H., Chen, L.-F., Wang, Z.-F., Wang, J., Tao, J.-H., and Wang, X.-H.: Did the widespread haze pollution over China increase during the last decade? A satellite view from space, Environ. Res. Lett., 11, 054019, https://doi.org/10.1088/1748-9326/11/5/054019, 2016.

Wang. L. and Chen, W.: An intensity index for the East Asian Winter Monsoon, J. Climate, 27, 2361–2374, https://doi.org/10.1175/JCLI-D-13-00086.1, 2014.

Wang, B., Wu, R.-G., and Fu, X.-H.: Pacific–East Asian teleconnection: how does ENSO affect East Asian climate?, J. Climate, 13, 1517–1536, https://doi.org/10.1175/1520-0442(2000)013<1517:PEATHD>2.0.CO;2, 2000.

Wang, Y.-S., Yao, L., Wang, L.-L., Liu, Z.-R., Ji, D.-S., Tang, G.-Q., Zhang, J.-K., Sun, Y., Hu, B., and Xin, J.-Y.: Mechanism for the formation of the January 2013 heavy haze pollution episode over central and eastern China, Sci. China Earth Sci., 57, 14–25, https://doi.org/10.1007/s11430-013-4773-4, 2014a.

Wang, Z.-F., Li, J., Wang, Z., Yang, W.-Y., Tang, X., Ge, B.-Z., Yan, P.-Z., Zhu, L.-L., Chen, X.-S., Chen, H.-S., Wand, W., Li, J.-J., Liu, B., Wang, X.-Y., Wand, W., Zhao, Y.-L., Lu, N., and Su, D.-B.: Modeling study of regional severe hazes over mid-eastern China in January 2013 and its implications on pollution prevention and control, Sci. China Earth Sci., 57, 3–13, https://doi.org/10.1007/s11430-013-4793-0, 2014b.

Wang, H.-J., Chen, H.-P., and Liu, J.-P.: Arctic sea ice decline intensified haze pollution in eastern China, Atmos. Ocean. Sci. Lett., 8, 1–9, https://doi.org/10.3878/AOSL20140081, 2015a.

Wang, Z.-L., Zhang, H., and Zhang, X.-Y.: Projected responses of East Asian Summer Monsoon system to future reductions in emissions of anthropogenic aerosols and their precursors, Clim. Dynam., 47, 1455–1468, https://doi.org/10.1007/s00382-015-2912-7, 2015b.

Wu, T.-W., Yu, R.-C., Zhang, F., Wang, Z.-Z., Dong, M., Wang, L.-N., Jin, X., Chen, D.-L., and Li, L.: The Beijing Climate Center atmospheric general circulation model: description and its performance for the present-day climate, Clim. Dynam., 34, 123–147, https://doi.org/10.1007/s00382-008-0487-2, 2010.

Wu, R.-G., Wen, Z.-P., and He, Z.-Q.: ENSO contribution to aerosol variations over the Maritime Continent and the Western North Pacific during 2000–10, J. Climate, 26, 6541–6560, https://doi.org/10.1175/JCLI-D-12-00253.1, 2013.

Yan, L.-P., Liu, X.-D., Yang, P., Yin, Z.-Y., and North, G. R.: Study of the impact of summer monsoon circulation on spatial distribution of aerosols in East Asia based on numerical simulation, J. Appl. Meteorol. Clim., 50, 2270–2282, https://doi.org/10.1175/2011JAMC-D-11-06.1, 2011.

Yang, Y., Liao, H., and Li, J.: Impacts of the East Asian summer monsoon on interannual variations of summertime surface-layer ozone concentrations over China, Atmos. Chem. Phys., 14, 6867–6879, https://doi.org/10.5194/acp-14-6867-2014, 2014.

Zhai, P.-M., Yu, R., Guo, Y.-J., Li, Q.-X., Ren, X.-J., Wang, Y.-Q., Xu, W.-H., Liu, Y.-J., and Ding, Y.-H.: The strong El Niño of 2015/16 and its dominant impacts on global and China's climate, J. Meteorol. Res.-P.R.C., 30, 283–297, https://doi.org/10.1007/s13351-016-6101-3, 2016.

Zhang, Y.-L. and Cao, F.: Fine particulate matter ($PM_{2.5}$) in China at a city level, Sci. Rep., 5, 14884, https://doi.org/10.1038/srep14884, 2015.

Zhang, R.-H., Sumi, A., and Kimoto, M.: A diagnostic study of the impact of El Niño on the precipitation in China, Adv. Atmos. Sci., 16, 229–241, https://doi.org/10.1007/BF02973084, 1999.

Zhang, L., Liao, H., and Li, J.-P.: Impacts of Asian Summer Monsoon on seasonal and interannual variations of aerosols over eastern China, J. Geophys. Res., 115, D716, https://doi.org/10.1029/2009JD012299, 2010.

Zhang, H., Wang, Z.-L., Wang, Z.-Z., Liu, Q.-X., Gong, S.-L., Zhang, X.-Y., Shen, Z.-P., Lu, P., Wei, X.-D., Che, H.-Z., and Li, L.: Simulation of direct radiative forcing of aerosols and their effects on East Asia climate using an interactive AGCM-aerosol coupled system, Clim. Dynam., 38, 1675–1693, https://doi.org/10.1007/s00382-011-1131-0, 2012a.

Zhang, X. Y., Wang, Y. Q., Niu, T., Zhang, X. C., Gong, S. L., Zhang, Y. M., and Sun, J. Y.: Atmospheric aerosol compositions in China: spatial/temporal variability, chemical signature, regional haze distribution and comparisons with global aerosols, Atmos. Chem. Phys., 12, 779–799, https://doi.org/10.5194/acp-12-779-2012, 2012b.

Zhang, H., Xie, B., Zhao, S.-Y., and Chen, Q.: $PM_{2.5}$ and tropospheric O_3 in China and an analysis of the impact of pollutant emission control, Adv. Clim. Change Res., 5, 136–141, https://doi.org/10.1016/j.accre.2014.11.005, 2014a.

Zhang, R.-H., Li, Q., and Zhang, R.-N.: Meteorological conditions for the persistent severe fog and haze event over eastern China in January 2013, Sci. China Earth Sci., 57, 26–35, https://doi.org/10.1007/s11430-013-4774-3, 2014b.

Zhang, H., Zhao, S.-Y., Wang, Z.-L., Zhang, X.-Y., and Song, L.-C.: The updated effective radiative forcing of major anthropogenic aerosols and their effects on global climate at present and in the future, Int. J. Climatol., 36, 4029–4044, https://doi.org/10.1002/joc.4613, 2016.

Zhao, S.-Y., Zhi, X.-F., Zhang, H., Wang, Z.-L., and Wang, Z.-Z.: Primary assessment of the simulated climatic state using a coupled aerosol-climate model BCC_AGCM2.0.1_CAM, Clim. Environ. Res., 19, 265–277, https://doi.org/10.3878/j.issn.1006-9585.2012.12015, 2014 (in Chinese).

Zhao, S.-Y., Chen, L.-J., and Cui, T.: Effects of ENSO phase-switching on rainy-season precipitation in north China, Chinese J. Atmos. Sci., 41, 857–868, https://doi.org/10.3878/j.issn.1006-9895.1701.16226, 2017 (in Chinese).

Zhu, J.-L., Liao, H., and Li, J.-P.: Increases in aerosol concentrations over eastern China due to the decadal-scale weakening of the East Asian Summer Monsoon, Geophys. Res. Lett., 39, L09809, https://doi.org/10.1029/2012GL051428, 2012.

Zou, Y.-F., Wang, Y.-H., Zhang, Y.-Z., and Koo, J.-H.: Arctic sea ice, Eurasia snow, and extreme winter haze in China, Sci. Adv., 3, e1602751, https://doi.org/10.1126/sciadv.1602751, 2017.